Available online at www.sciencedirect.com

SciVerse ScienceDirect

Ceramics International 39 (2013) 731–736

CERAMICS INTERNATIONAL

www.elsevier.com/locate/ceramint

Fabrication and microstructure of *in situ* vanadium carbide ceramic particulates-reinforced iron matrix composites

Lisheng Zhong[a,b], Mirabbos Hojamberdiev[b,*], Fangxia Ye[b], Hong Wu[b], Yunhua Xu[a,b,**]

[a]*School of Mechanical and Electrical Engineering, Xi'an University of Architecture and Technology, Xi'an 710055, PR China*
[b]*Institute of Wear Resistant Materials, Xi'an University of Architecture and Technology, Xi'an 710055, PR China*

Received 30 April 2012; received in revised form 29 May 2012; accepted 26 June 2012
Available online 4 July 2012

Abstract

In this work, a novel process that combines infiltration casting with subsequent heat treatment was applied to fabricate *in situ* vanadium carbide (V_8C_7) ceramic particulates-reinforced iron matrix composites. Based on the differential scanning calorimetry (DSC) data, the as-cast samples were subjected to heat treatment at 1164 °C for different dwelling times (0, 10, 15, and 20 min). The effects of different heat treatment times on the phase evolution, microstructure, and microhardness of the as-prepared composites were investigated using X-ray diffraction (XRD), scanning electron microscope (SEM), energy dispersive X-ray spectrometer (EDS), and Vickers hardness tester, respectively. The experimental results revealed that only graphite, α-Fe, and V_8C_7 phases dominate in the composite samples after heat treatment at 1164 °C for 20 min. The average microhardness of the as-prepared composites varied among the different regions as follows: 458 $HV_{0.05}$ (vanadium wire), 1055 $HV_{0.05}$ (composite area), and 235 $HV_{0.05}$ (iron matrix). The microhardness of the composite region is four times higher than that of the iron matrix and two times higher than that of the vanadium wire because of the formation of the vanadium carbide phases (V_2C and V_8C_7) as reinforcement within the iron matrix.

Keywords: A. Joining; B. Composites; C. Hardness; D. Carbides

1. Introduction

Metal matrix composites (MMCs) are a unique class of engineering materials in which a rigid ceramic reinforcement is incorporated into a metal matrix. As previously demonstrated [1], MMCs combine the metallic properties of matrix alloys (ductility and toughness) with the ceramic properties of the reinforcements (high strength and high modulus). Although extensive work has been done on the production of novel and lightweight metal matrix composites, increasing attention has focused on developing iron and steel matrix composites because of their simple processing, low cost, and isotropic properties. Thus far, the methods commonly applied in manufacturing reinforced MMCs are casting, self-propagating high-temperature synthesis, powder metallurgy, and *in situ* reaction. Kambakas and Tsakiropoulos [2] demonstrated a casting technique for producing materials with wear-resistant surfaces, which consist of a white cast iron matrix reinforced with *ex situ*- and *in situ*-formed transition and refractory metal carbide ceramic particulates. Persson et al. [3] applied liquid-phase sintering (LPS) and self-propagating high-temperature synthesis (SHS) to manufacture highly reinforced TiC/Fe composites. Wang et al. [4–6] reported a novel process that combines *in situ* synthesis with powder metallurgy technique to produce (Ti,V)C/Fe matrix composites. Other authors [7–9] also reported the fabrication of reinforced MMCs using an *in situ* reaction method. However, the production of reinforced MMCs through various casting technologies has two major shortcomings. First, the segregation of reinforcement particulates in the iron matrix is likely to be uneven because of the

*Corresponding author. Present address: Materials and Structures Laboratory, Tokyo Institute of Technology, 4259 Nagatsuta, Midori, Yokohama, Kanagawa 226-8503, Japan.
**Corresponding author at: School of Mechanical and Electrical Engineering, Xi'an University of Architecture and Technology, Xi'an 710055, PR China. Tel.: +86 29 82202718; fax: +86 29 82207898.
E-mail addresses: hmirabbos@gmail.com (M. Hojamberdiev), yunhuaxu@yahoo.com.cn (Y. Xu).

0272-8842/$36.00
http://dx.doi.org/10.1016/j.ceramint.2012.06.085

density difference between the matrix and the reinforcement. Second, the volume fraction of the reinforcement is limited because of the reduced fluidity of the matrix at high reinforcement levels. The ceramic particulate-reinforced MMCs produced using self-propagating high-temperature synthesis cannot be directly used as a structural material because of its porosity and looseness. Powder metallurgy is based on the addition of ceramic reinforcements to matrix materials prepared separately prior to composite fabrication. As a result, interfacial reactions and poor wettability occur between the matrix and the reinforcements, which are caused by surface contamination of the reinforcements. Therefore, the *in situ* route is considered one of the most promising methods because the *in situ*-formed reinforcements are thermodynamically stable at the matrix and the reinforcement-matrix interfaces are relatively clean, resulting in strong interfacial bonding. Additionally, the reinforcing ceramic particles have finer sizes and more uniform distributions in the matrix compared with *ex situ*-prepared MMCs [5]. By applying *in situ* synthesis, TiC [10–12], WC [13,14], and VC [15–17] were prepared by a combination of casting, self-propagating high-temperature synthesis, and powder metallurgy.

Vanadium carbide (VC) with the microhardness value of 2460–3150 $HV_{0.05}$ can be employed to reinforce an iron-based matrix, leading to a significant improvement in abrasion performance [5]. Most importantly, the standard free energy for the formation of vanadium carbide is lower and wettability indicated by the smaller contact angle θ of 28° between the vanadium carbide and the iron matrix is better. Previously, vanadium carbide dispersions were *in situ* generated in melt steel alloys, and the volume fraction of carbides of up to 14% was reported with carbide particle size in the range of 3–10 μm [16]. An iron-based surface composite reinforced with vanadium carbide ceramic particles was produced by a metal-coated casting technique, and the volume fraction of vanadium carbide ceramic particles was up to 39.5% with particle sizes in the range of 1–3 μm [17]. The above-listed results demonstrated that an *in situ* synthesis route would be favorable for fabricating the iron-based composites reinforced with the vanadium carbide ceramic particulates. However, those results were obtained by combined methods, *i.e. in situ* reaction with powder metallurgy and *in situ* reaction with cast sintering, having the advantages of a nearly perfect surface quality and high precision of final products. Nevertheless, the fabricated products were monolithic composites with a high production cost, restricted shape and size. Also, the scale of reinforcing phase was limited by the size of starting powders.

The purpose of the present work is to fabricate the *in situ* vanadium carbide ceramic particulates-reinforced iron matrix composites by a novel process combining infiltration casting with subsequent heat treatment. The effects of different heat treatment times at 1164 °C on the phase evolution, microstructure, and microhardness of the composites were systematically investigated in this study.

2. Experimental

2.1. Preparation

The starting materials were gray cast iron and vanadium wires (ϕ1 mm) with 99.99% purity. They were employed as carbon and vanadium sources for the *in situ* synthesis of vanadium carbide ceramic particulates within the iron matrix. The chemical composition (wt%) of gray cast iron is Fe–4.22C–0.58Si–0.268Mn–0.224P–0.024S. First, a gray cast iron mold was produced in rectangular shape, as shown in Fig. 1a. A number of holes were inversely drilled (ϕ1 mm) on both sides of the mold (Fig. 1b), with the targeted distance of 3 mm between the holes. Then, the vanadium wires were passed through the drilled holes on both sides and firmly fixed with the mold (Fig. 1c). Later, the vanadium wire-fixed gray cast iron mold was inserted into a graphite mold (Fig. 1d). Molten gray cast iron was produced in a medium-frequency induction furnace and poured into the mold at 1430 °C. The specimen was immediately covered with quartz sand to avoid the crack generation and cooled down to room temperature. After that, the specimen was taken out of the graphite mold and cut in the size of 10 mm × 10 mm × 25 mm by a numerically controlled wire-cut EDM machine (Suzhou Nutac Electro Mechanic Co., Ltd., China). According to the differential scanning calorimetry (DSC) data, the sectioned samples were subjected to heat treatment at 1164 °C for different dwelling times (0, 10, 15, and 20 min) in a horizontal tube furnace with a modest flow of argon gas and cooled down to room temperature naturally.

2.2. Characterization

After being well polished with diamond paste and etched with a 4% Nital solution, the microstructures of specimens were examined using a JSM-5800 scanning electron

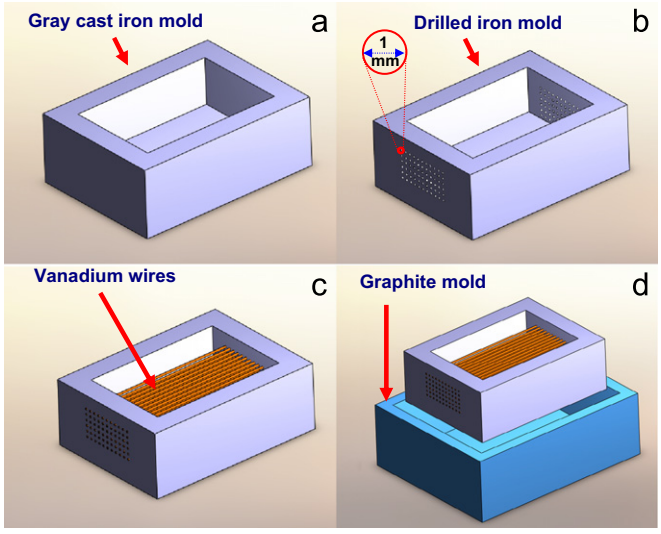

Fig. 1. 3D images of the gray cast iron mold (a), drilled mold (b), preform (c) and graphite mold (d) used in the experiment.

microscope (JEOL, Japan) equipped with an energy dispersive X-ray spectroscopy (EDS). The X-ray diffraction (XRD) data was recorded on a PW 1730 X-ray diffractometer (Philips, The Netherlands) with monochromated Cu Kα radiation at 40 kV and 40 mA in the 2θ range of 10–90°. The microhardness of specimens was measured using an HDX-1000 digital microhardness tester. The static load was 50 g for 15 s. An average value of microhardness was taken from at least five different measurements. To determine the pouring temperature of gray cast iron melt, differential scanning calorimetry (DSC)/thermogravimetric analysis (TGA) was performed on a Q600 SDT (TA Instruments, USA) for the cylindrical sample with the diameter of 2 mm and the height of 2.6 mm prepared from gray cast iron and vanadium wire. The sample was heated at a heating rate of 10 °C/min up to a maximum temperature of 1400 °C with a 150 ml/min flow rate of argon gas and cooled down to room temperature naturally.

3. Results and discussion

The DSC curve of the specimen is shown in Fig. 2. As shown in the figure, three main endothermic peaks are centered at 788 °C, 808 °C, and 1164 °C, and one exothermic peak is centered at 1347 °C. The endothermic peaks at 788 °C, 808 °C, and 1164 °C are attributed to an allotropic change α-Fe→γ-Fe, β-V_2C→α-V_2C+β-V_2C, and the ternary eutectic transformation L→γ-Fe+graphite+V_8C_7 [4,18], respectively. The exothermic peak at 1347 °C is related to the formation of vanadium carbides by the reaction (L→γ-Fe+VC_x) between the carbon in the iron matrix and the vanadium in the wire. The reaction that occurs near the ternary eutectic transformation is conducive to graphite precipitation, and is beneficial to maintaining matrix consistency. Based on the DSC data, 1164 °C was chosen as the optimum temperature for further heat treatment of the as-cast samples.

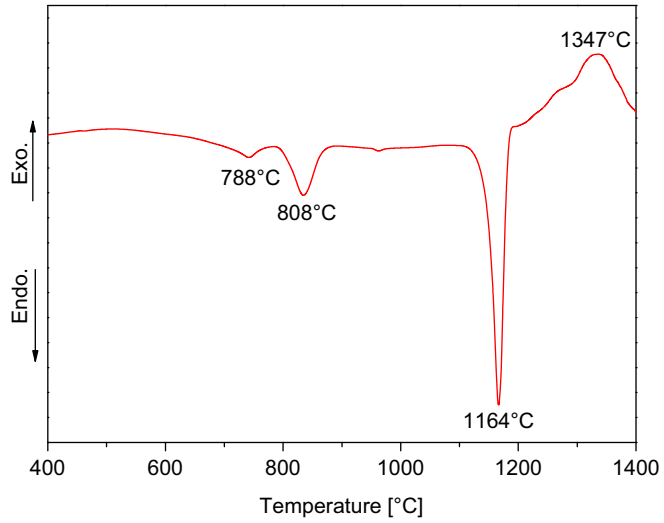

Fig. 2. DSC curve of the specimen.

The SEM micrographs of the *in situ* vanadium carbide ceramic particulates-reinforced iron matrix composites are shown in Fig. 3 as a function of heat treatment time. Figs. 3a–d show that the diffused region broadens gradually with increasing heat treatment time from 0 min to 20 min, and the diameter of a metallic vanadium wire contracts and eventually disappears. Between the vanadium wire and the iron matrix, the composite region was divided into three apparent concentric circles (regions) after heat treatment at 1164 °C. The three regions were denoted as A, B, and C, as shown in Fig. 3b, where the diffusion reaction mainly took place. Fig. 3d shows the SEM micrograph of the composite region of the specimen heat treated at 1164 °C for 20 min. The vanadium wire was completely melted and more vanadium atoms diffused into the iron matrix. The diameter of the *in situ* reaction region was extended to 1.3 mm, which is higher than those of the original vanadium wires. The *in situ* reaction region was clearly joined firmly to the iron matrix without apparent defects.

The XRD patterns of the *in situ* vanadium carbide ceramic particulates-reinforced iron matrix composites are shown in Fig. 4 with different heat treatment times. It is clear that the graphite, vanadium, α-Fe, V_2C and V_8C_7 dominate as main crystalline phases in the specimens after heat treatment at 1164 °C for 0–15 min. Only graphite, α-Fe and V_8C_7 become dominating phases in the specimen after heat treatment at 1164 °C for 20 min. A sudden disappearance of the vanadium diffraction peaks after heat treatment at 1164 °C for 20 min confirms that all metallic vanadium atoms were consumed for the reaction with graphite in the iron matrix, and a decent amount of unreacted graphite is still present in the composite specimen. Hence, the vanadium carbide (V_8C_7)—dominated iron matrix composites could be obtained under the current

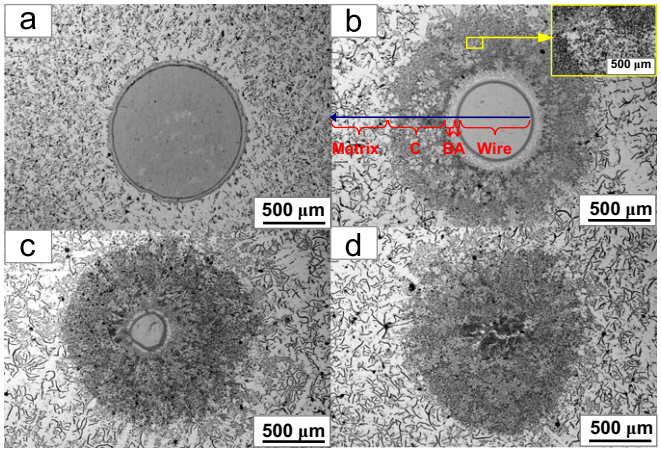

Fig. 3. SEM micrographs of the *in situ* vanadium carbide ceramic particulates-reinforced iron matrix composites heat treated at 1164 °C for 0 min (a), 10 min (b), 15 min (c), and 20 min (d). Keys: Wire—vanadium wire; A, B, and C—total composite regions and Matrix—iron matrix. An inset represents the iron enrichment zone in region C of a composite area.

experimental conditions along with a decent amount of unreacted graphite.

To obtain more information on the regions A, B, and C in the composite, the specimens were examined by scanning electron microscopy and energy dispersive X-ray spectroscopy. The SEM micrographs and EDS spectra are illustrated in Fig. 5. According to the EDS results obtained from the crystalline particles present in each region, the ratio of vanadium to carbon is 1:0.54, 1:0.86, and 1:0.94 for the regions of A, B, and C, respectively, in the specimen heat treated at 1164 °C for 10 min. By comparing with XRD results, these values are considered to be close to the atomic ratio of V_2C and V_8C_7, respectively. The microstructures of the regions A, B and C show the presence of short-regional V_2C crystals, agglomerated irregular V_8C_7 crystals, and spherical and rod-like V_8C_7 crystals in the iron matrix. The crystalline

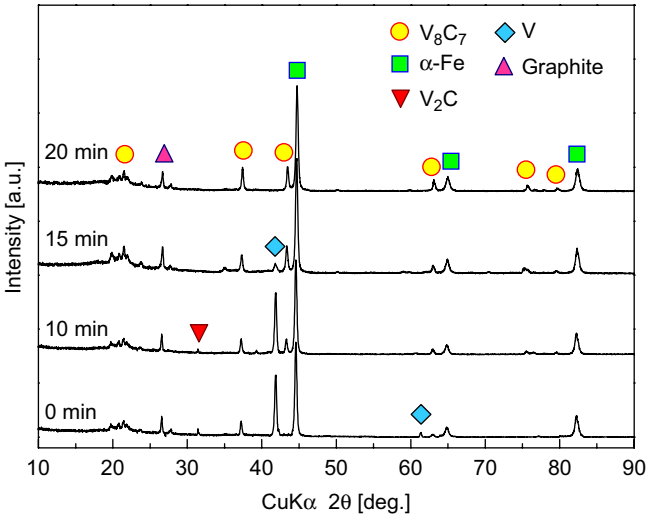

Fig. 4. XRD patterns of the *in situ* vanadium carbide ceramic particulates-reinforced iron matrix composites as a function of heat treatment time.

V_8C_7 particles are uniformly dispersed in the iron matrix in regions B and C. The particulate size of V_8C_7 in region B (1–3 μm) is smaller than that of V_8C_7 in region C (2–5 μm). This evidences that the V_8C_7 crystallites grow with the prolongation of heat treatment time. We also observed the iron enrichment zone in region C, as shown in inset of Fig. 3b, and however, its exact formation needs further investigations.

Generally, in the ternary Fe–V–C system, vanadium can easily react with carbon at high temperature to form VC_x, which is carbide with a vacancy in the VC, and the quantity of carbon atoms is about 0.50–0.96. The region of homogeneity is wide, and within this region the disordered VC_x crystallizes in the NaCl-type cubic structure. Nevertheless, the stoichiometric composition of $VC_{1.00}$ cannot be obtained under the equilibrium conditions. In previous reports [19–21], ordered cubic phase V_8C_7, V_6C_5, V_4C_3, V_2C were obtained, and the lattice parameters were twice as large as those of disordered carbide. In this study, only V_8C_7 and V_2C phases were formed in the iron matrix. The main reason might be related to the variance of local concentration at different regions. Near the vanadium wire, the concentration of the vanadium atoms was much higher than that of carbon atoms because the carbon diffusion was inhibited by the reaction products; so, the V_2C could form due to a low carbon–vanadium ratio. In contrast, outside the region A, the amount of carbon atoms was superfluous, and the V_8C_7 crystallites formed readily in regions B and C owing to the higher carbon–vanadium ratio.

Microhardness distribution in the composite region of the as-prepared composite specimen heat treated at 1164 °C for 10 min is plotted in Fig. 6 as a function of the distance from the center of reinforcement phase to the iron matrix. As shown in Fig. 6, the highest microhardness value (1896 $HV_{0.05}$) is obtained from the diffusion reaction region A due to the presence of intensive V_2C ceramic particles. However, the highest microhardness value still

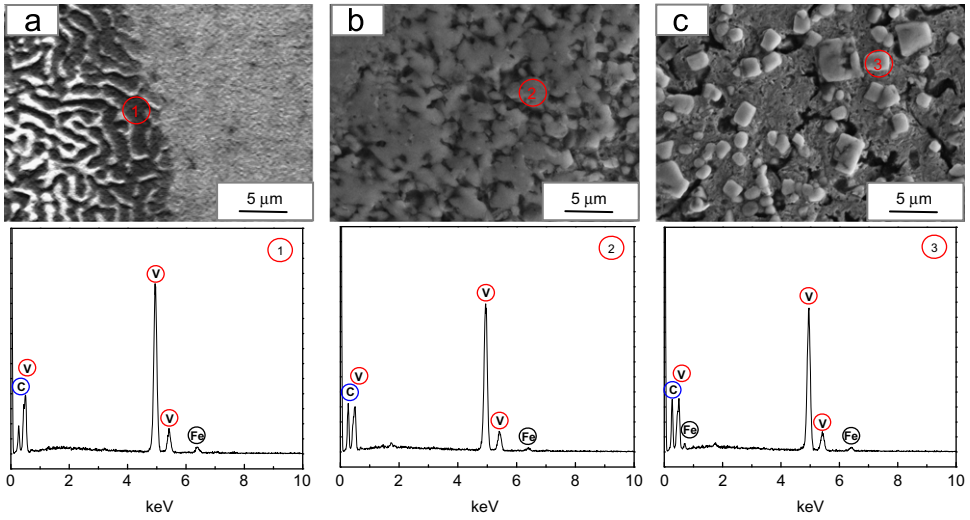

Fig. 5. SEM micrographs and EDS spectra of the regions A (a), B (b) and C (c) of the specimen heat treated at 1164 °C for 10 min.

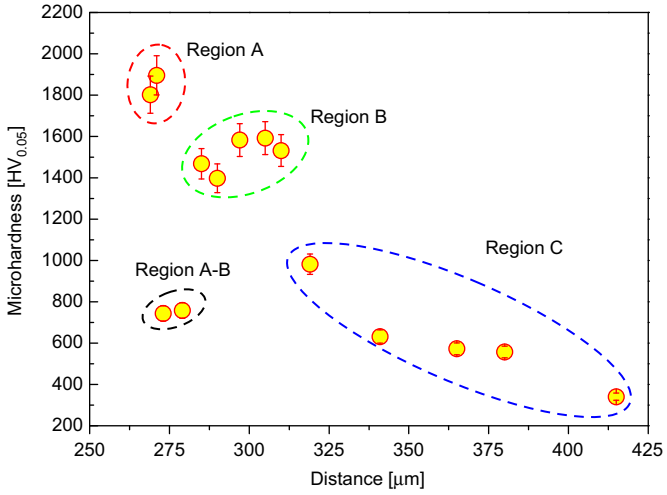

Fig. 6. Microhardness distribution in the total composite region of the specimen heat treated at 1164 °C for 10 min as a function of the distance from the center of reinforcement phase to the iron matrix.

could not reach the theoretical value (2460–3150 $HV_{0.05}$) for the vanadium carbide because the particle size of the V_2C is too small compared with a tip of diamond-shaped indenter; moreover, the ceramic particles might be slightly moved during the test. Unexpectedly, there is an abrupt reduction in microhardness value (744–758 $HV_{0.05}$) between the regions A and B. Probably, the reason might be the presence of less amount of carbon and vanadium in the transformation area between the regions A and B, and therefore, the vanadium carbide formation might have been limited in this iron-rich region. The microhardness value goes up again in region B and that trend subsequently falls down to 341 $HV_{0.05}$ in region C. Although the presence of V_8C_7 crystallites in regions B and C, the microhardness values are quite different. This can be related to the formation of V_8C_7 particles with a specific morphology in each region. That is, in region B the V_8C_7 particles were formed with highly agglomerated morphology while the V_8C_7 particles were formed separately in region C. We believe that the indentation in region C might have taken place randomly either on a smaller V_8C_7 particle or directly on the iron matrix, which gave lower microhardness values. In short, the average microhardness values of the main regions can be placed in the following order: 235 $HV_{0.05}$ (iron matrix) < 458 $HV_{0.05}$ (vanadium wire) < 1055 $HV_{0.05}$ (composite area). It is clear that the average microhardness value of the composite region is four times higher than that of the iron matrix and two times higher than that of the vanadium wire.

According to the standard thermodynamic calculations [22,23], the following possible reactions might have taken place in the Fe–V–C system:

$$2V+C=V_2C \quad \Delta G_1=-146.4-0.00634T(kJ/mol) \times(273^\circ C<T<1727^\circ C)$$

$$8V+7C=V_8C_7$$

$$\Delta G_2=-98.7+1.26\times10^{-3}T\ln T+0.835\times10^{-6}T^2+0.83\times10^2T^{-1}-1.08\times10^{-3}T(kJ/mol)(273^\circ C<T<1727^\circ C)$$

$$3Fe(\alpha)+C(gr)=Fe_3C(s) \quad \Delta G_3=-38.05+0.0571T(25^\circ C<T<190^\circ C)$$

$$3Fe(\gamma)+C(gr)=Fe_3C(s) \quad \Delta G_4=-37.3+0.1050T(25^\circ C<T<842^\circ C)$$

$$3Fe(\delta)+C(gr)=Fe_3C(s) \quad \Delta G_5=-53.64+0.06995T(842^\circ C<T<1454^\circ C)$$

The Gibbs free energies (ΔG) calculated for the V_2C, V_8C_7 and Fe_3C are plotted in Fig. 7 as a function of temperature. From Fig. 7, it can be noticed that the vanadium has a stronger carbide forming tendency than iron. The V_2C and V_8C_7 phases are stable carbides, and their Gibbs free energies do not change significantly with temperature. As expected, the Gibbs free energies for the formation of the V_2C and V_8C_7 phases are negative, which confirms the favorable reaction at the temperature used in this work. In the range of heat treatment time of 0–15 min, the V_2C could be formed around the vanadium wire, and after heat treatment for 20 min the V_8C_7 could be formed as a predominant phase in the gray cast iron matrix. Although the difference in the space group and lattice parameters, the V_2C and V_8C_7 have similar atomic arrangements if the carbon vacancies are not taken into account. The only difference is that the quantity of carbon vacancies in the V_2C is more than that in the V_8C_7. Aouni et al. [24] elaborated that when there are enough carbon atoms to fill the vacancies, the V_2C would transfer to other structure. In this study, the concentration of carbon atoms in the composite region (A, B, and C) was increased with increasing heat treatment time. According to the Fick's second law of diffusion, higher carbon–vanadium ratio was beneficial to form V_8C_7 compare to V_2C, because more carbons could fill carbon vacancies. More carbon atoms were present in the iron matrix than vanadium

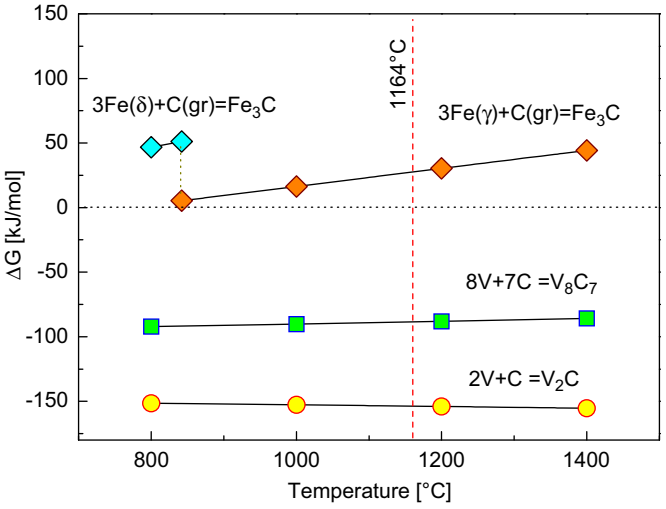

Fig. 7. Gibbs free energies for the V_2C, V_8C_7 and Fe_3C phases as a function of temperature.

atoms after heat treatment at 1164 °C for 20 min, so the V_2C phase could be completely transformed into the V_8C_7 phase.

4. Conclusions

In summary, the *in situ* vanadium carbide (V_8C_7) ceramic particulates-reinforced iron matrix composites were fabricated using a novel process combining an infiltration casting process with subsequent heat treatment. The effects of different heat treatment times (0, 10, 15, and 20 min) at 1164 °C on the phase evolution, microstructure, and microhardness of the *in situ* vanadium carbide ceramic particulate-reinforced iron matrix composites were investigated. The XRD results showed that only graphite, α-Fe, and V_8C_7 dominated in the composite after heat treatment at 1164 °C for 20 min. The SEM observations revealed the presence of short-regional V_2C, agglomerated irregular V_8C_7, and spherical and rod-like V_8C_7 particles in the iron matrix for composite regions A, B, and C, respectively. The average microhardness of the as-prepared composites varied from region to region, as follows: 458 $HV_{0.05}$ (vanadium wire), 1055 $HV_{0.05}$ (composite area), and 235 $HV_{0.05}$ (iron matrix). The microhardness of the composite area was four times higher than that of the iron matrix and two times higher than that of vanadium wire because of the formation of crystalline vanadium carbides (V_2C and V_8C_7) as reinforcement phases in the iron matrix.

Acknowledgment

The present work was financially supported by a grant from the National Natural Science Foundation of China (No. 50974101).

References

[1] S.C. Tjong, Z.Y. Ma, Microstructural and mechanical characteristics of *in situ* metal matrix composites, Materials Science and Engineering Reports 29 (2000) 49–113.
[2] K. Kambakas, P. Tsakiropoulos, Sedimentation casting of wear resistant metal matrix composites, Materials Science and Engineering A 435–436 (2006) 187–192.
[3] P. Persson, A.E.W. Jarfors, S. Savage, Self-propagating high-temperature synthesis and liquid-phase sintering of TiC/Fe composites, Journal of Materials Processing Technology 127 (2002) 131–139.
[4] J. Wang, Study on the Mechanical Properties of (Ti,V)C/Fe Produced by *in situ* Synthesis, Ph.D. Thesis, Sichuan University, China, 2007 (in Chinese).
[5] J. Wang, Y. Wang, Y. Ding, W. Gong, Microstructure and wear-resistance of Fe–(Ti,V)C composite, Materials and Design 28 (2007) 2207–2209.
[6] W. Jing, W. Yisan, D. Yichao, Reaction synthesis of Fe–(Ti,V)C composites, Journal of Materials Processing Technology 197 (2008) 54–58.
[7] Z. Mei, Y.W. Yan, K. Cui, Effect of matrix composition on the microstructure of *in situ* synthesized TiC particulate reinforced iron-based composites, Materials Letters 57 (2003) 3175–3181.
[8] J.-L. Ji, J.-L. Tang, Wear-corrosion behavior of cast-in composite materials reinforced by WC particles, Wear 138 (1990) 23–32.
[9] Y. Wang, Z. Sun, Y. Ding, Z. Li, *In situ* production of VC–SiO_2–Fe surface composite by cast-sintering, Materials and Design 25 (2004) 69–72.
[10] K.S. Ashok, D. Karabi, Microstructural and mechanical characterization of *in situ* TiC and (Ti,W)C-reinforced high manganese austenitic steel matrix composites, Materials Science and Engineering A 516 (2009) 1–6.
[11] C. Cui, Z. Guo, H. Wang, J.J. Hu, *In situ* TiC particles reinforced grey cast iron composite fabricated by laser cladding of Ni–Ti–C system, Journal of Materials Processing Technology 183 (2007) 380–385.
[12] R.K. Galgali, H.S. Ray, A.K. Chakrabarti, Wear characteristics of TiC reinforced cast iron composites part 1—adhesive wear, Materials Science and Technology 14 (1998) 810–815.
[13] C. Wei, X. Song, S. Zhao, L. Zhang, W. Liu, *In-situ* synthesis of WC–Co composite powder and densification by sinter-HIP, International Journal of Refractory Metals and Hard Materials 28 (2010) 567–571.
[14] G.-S. Zhang, J.-D. Xing, Y.-M. Gao, Impact wear resistance of WC/Hadfield steel composite and its interfacial characteristics, Wear 260 (2006) 728–734.
[15] Y. Wang, X. Zhang, G. Zeng, F. Li, *In situ* production of Fe–VC and Fe–TiC surface composites by cast-sintering, Composites Part A 32 (2001) 281–286.
[16] R.S. Tittagala, P.R. Beeley, A.N. Bramley, Evaluation of some new cast hot-work die steels using simulation wear test, Metal Technology 10 (1983) 257–261.
[17] Y. Wang, F. Li, G. Zeng, D. Feng, Structure and wear-resistance of an Fe–VC surface composite produced *in situ*, Materials and Design 20 (1999) 19–22.
[18] A.I.Z. Farahat, Dilatometry determination of phase transformation temperatures during heating of Nb bearing low carbon steels, Journal of Materials Processing Technology 204 (2008) 365–369.
[19] V.N. Lipatnikov, W. Lengauer, P. Ettmayer, E. Keil, G. Groboth, E. Kny, Effects of vacancy ordering on structure and properties of vanadium carbide, Journal of Alloys and Compounds 261 (1997) 192–197.
[20] A.M. Henfrey, B.E.F. Fender, A neutron diffraction investigation of V_8C_7, Acta Crystallographica B 26 (1970) 1882–1883.
[21] K. Feng, M. Hong, Y. Yang, W. Wang, Combustion synthesis of VC/Fe composites under the action of an electric field, International Journal of Refractory Metals and Hard Materials 27 (2009) 852–857.
[22] C.C. Wu, Thermodynamics of Metallurgical Processes, China Machine Press, Beijing, 1993 pp.194–199 (in Chinese).
[23] Y. Ding, Y. Wang, J. Wang, Y. Xian, Structure and properties of V_8C_7 matrix composite fabricated *in-situ*, Journal of Sichuan University 39 (2007) 113–117.
[24] A. Aouni, P. Weisbecker, T.H. Loi, E. Bauer-Grosse, Search for new materials in sputtered $V_{1-x}C_x$ films, Thin Solid Films 469–470 (2004) 315–321.